THE JOURNAL OF PHYSICAL CHEMISTRY B

Article

Effect of Functionalization of Multiwalled Nanotubes on the Crystallization and Hydrolytic Degradation of Biodegradable Poly(l-lactide)

Yuanyuan Zhao, Zhaobin Qiu, and Wantai Yang

J. Phys. Chem. B, **2008**, 112 (51), 16461-16468 • Publication Date (Web): 04 December 2008

Effect of Functionalization of Multiwalled Nanotubes on the Crystallization and Hydrolytic Degradation of Biodegradable Poly(L-lactide)

Yuanyuan Zhao, Zhaobin Qiu,* and Wantai Yang

State Key Laboratory of Chemical Resource Engineering, Beijing University of Chemical Technology, Beijing 100029, China

Received: June 13, 2008; Revised Manuscript Received: September 10, 2008

Biodegradable poly(L-lactide) (PLLA)/multiwalled carbon nanotubes (MWNTs) nanocomposites were prepared via solution blending using two kinds of MWNTs, i.e., pristine multiwalled carbon nanotubes (p-MWNTs) and carboxyl-functionalized multiwalled carbon nanotubes (f-MWNTs). Various techniques were used to investigate the functionalization of MWNTs on the morphology, crystallization, and hydrolytic degradation of PLLA in the nanocomposites. Both MWNTs show fine dispersion in the PLLA matrix; however, the dispersion of f-MWNTs is better than that of p-MWNTs. The incorporation of MWNTs accelerates the crystallization of PLLA in the nanocomposites due to the heterogeneous nucleation effect; furthermore, the crystallization rate of PLLA is faster in the PLLA/f-MWNTs nanocomposite than in the PLLA/p-MWNTs nanocomposite. The exciting aspect of this research is that the hydrolytic degradation of PLLA is enhanced after nanocomposites preparation.

Introduction

Carbon nanotubes (CNTs) were first reported by Iijima in 1991,[1] which possess high flexibility, low mass density, and large aspect ratio,[2] and have a unique combination of mechanical, electrical, and thermal properties that make nanotubes excellent candidates to substitute or complement the conventional nanofillers in the fabrication of multifunctional polymer nanocomposites.[3−6] Many efforts have been directed at the fabrication of carbon nanotubes/polymer nanocomposites and the characterization of their physical properties. However, two main challenges still exist for developing high-performance CNTs/polymer nanocomposites.[7] The first challenge is how to improve the dispersion of CNTs in the polymer matrix, which is of great use for modifying the physical properties of polymer matrix. The second one is how to obtain the efficient translation of nanotube properties into the polymer matrix. There are several main methods reported for solving the matters: (1) high-power ultrasonication,[8,9] (2) high temperature and high shear forces in melt blending,[10] and (3) functionalization of carbon nanotubes,[11−14] which were utilized to improve dispersion and interfacial adhesion to the polymer matrix. Consequently, various properties of the CNTs/polymer nanocomposites were obviously improved.

Among studies on CNTs/polymer nanocomposites, nanocomposites comprising CNTs and the biodegradable polymers are of special interest due to their potential for specific biomaterial applications.[15−18] Poly(L-lactide) (PLLA) has attracted much attention because it is biodegradable, biocompatible, producible from renewable resources, and nontoxic to the human body and the environment. Recent innovation on the production process has lowered significantly the production cost, which further stimulates the studies on its property and potential applications.[19] However, its relatively poor mechanical properties, slow crystallization rate, and slow degradation rate have limited its wide practical application. To overcome the aforementioned problems, the preparation of its nanocomposites with CNTs may be a suitable and convenient way.[20−24] Moon et al. prepared PLLA/MWNTs nanocomposites by a solution casting method.[20] The mechanical and thermal properties as well as the electrical conductivity of nanocomposites were investigated. It was found that the tensile strength and ultimate elongation decreased, but Young's modulus slightly increased from 1 to 2.5 GPa. Zhang et al. reported the preparation of the PLLA/MWNTs nanocomposite, and the corresponding Raman spectroscopic and the microscopic characterization.[21] The electronic transport, thermal properties, and biocompatibility of the nanocomposite were also investigated. The cell culture test results suggested that the presence of MWNTs in the nanocomposite inhibited the growth of the fibroblast cells. Wu et al. prepared the PLLA/MWNTs hybrids via a melt blending method.[22] The results demonstrated dramatic enhancement in thermal properties of PLLA. Shieh et al. prepared films of the PLLA/MWNTs-*g*-PLLA nanocomposites by a solution casting method to investigate the effects of the MWNTs-*g*-PLLA on the nonisothermal and isothermal melt crystallizations of the PLLA matrix.[23] It was found that MWNTs significantly enhanced both nonisothermal melt and cold crystallization rates of PLLA. Kim et al. prepared the PLLA/PLLA-*g*-MWNTs nanocomposites by a melt-mixing method.[24] The morphology, mechanical properties, and thermal stability of the nanocomposites were studied by scanning electron microscopy, tensile test, and thermogravimetric analysis. It was found that the activation energy of thermal degradation of PLLA/PLLA-g- MWNTs was higher than that of PLLA/MWNTs, indicating that the former was more thermally stable than the latter. The results also showed that the addition of CNTs improved the mechanical, electrical, and thermal properties of PLLA.

In this work, PLLA/MWNTs nanocomposites were prepared via solution blending using chloroform as a mutual solvent. Two kinds of MWNTs, i.e., pristine multiwalled carbon nanotubes (p-MWNTs) and carboxyl-functionalized multiwalled carbon nanotubes (f-MWNTs), were used in order to investigate the functionalization of MWNTs on the morphology, crystallization

* Corresponding author. E-mail: qiuzb@mail.buct.edu.cn. Fax: +86-10-64413161.

10.1021/jp805230e CCC: $40.75
Published on Web 12/04/2008

kinetics, and crystal structure of PLLA in the nanocomposites. Moreover, the hydrolytic degradation experiments were performed to study the effect of the incorporation of MWNTs in the polymer matrix on the degradation of PLLA.

Experimental Section

Materials. PLLA ($M_w = 2.06 \times 10^5$) was kindly provided by Biomer Co., Germany. Both p-MWNTs and f-MWNTs were purchased from Chengdu Institute of Organic Chemistry, Chinese Academy of Sciences. The diameter was around 30−50 nm with lengths ranging between 10 and 20 μm.

Purification of PLLA. The PLLA pellets were purified by dissolution in chloroform and subsequent precipitation in an excess of methanol. The precipitated PLLA was filtered and dried in a vacuum at 70 °C for 2 days.

Preparation of PLLA/MWNTs Nanocomposites. The PLLA/MWNTs nanocomposites were prepared through a solution mixing method. For the fabrication of nanocomposites, PLLA was mixed with the addition of 1 wt % p-MWNTs and f-MWNTs, respectively. A representative procedure is as follows. Chloroform was used as the mutual solvent. On the one hand, the appropriate amount of MWNTs was added into the chloroform. Then, the mixture was sonicated with a KQ 3200E ultrasonic generator to make a uniformly dispersed suspension. On the other hand, purified PLLA were placed into chloroform and stirred for 1 h to dissolve PLLA completely. Next, the PLLA solution was added to the MWNTs suspension, and sonication was continued, with stirring for 6 h. The PLLA/MWNTs solution was poured into a dish to evaporate the solvent at room temperature. The sample was further dried at 70 °C under vacuum for 3 days to remove the solvent completely.

For the wide X-ray diffraction study, both neat PLLA and its nanocomposites were first pressed into films with a thickness of around 0.5 mm on a hot stage at 190 °C and then transferred into a vacuum oven at 125 °C for 24 h.

For the hydrolytic degradation study, the samples were molded into films on a hot press under a pressure of 30 MPa at 185 °C, which were allowed to cool to ambient temperature naturally by switching off the power of the hot press. The thickness of the films was around 0.8 mm.

Characterizations. Morphology of PLLA/MWNTs nanocomposites was observed using a Hitachi S-4700 scanning electron microscope (SEM). All specimens were coated with gold before examination. Transmission electron microscopy (TEM) observation of MWNTs was performed with a Hitachi H-800 TEM instrument under an acceleration voltage of 200 kV. Thin sections (with thickness of about 50−70 nm) for TEM observations were cut from the as-prepared nanocomposites under cryogenic conditions (−80 °C) using a Leica EM FC6 ultramicrotome.

Thermal analysis was performed using a TA Instruments differential scanning calorimetry (DSC) Q100 with a Universal Analysis 2000. Indium was used for temperature calibration. All operations were performed under nitrogen purge, and the weight of the samples varied between 4 and 6 mg. In the case of nonisothermal melt crystallization, the sample was heated from the ambient temperature to 190 °C at a rate of 20 °C/min (first heating), held for 3 min to erase the previous thermal history, and then cooled to 20 °C at a cooling rate of 5 °C/min (first cooling). The sample was further heated to 190 °C again from 20 °C at a heating rate of 20 °C/min (second heating) to study the subsequent melting behavior. The crystallization peak temperature was obtained from the first cooling traces. The glass transition temperature and melting point temperature of neat PLLA and its nanocomposite were read from the second heating traces. In the case of isothermal melt crystallization experiment, the sample was heated from the ambient temperature to 190 °C at a rate of 40 °C /min, held for 3 min to erase any thermal history, cooled to crystallization temperature at a cooling rate of 60 °C/min, and held until the isothermal crystallization was over. The crystallization temperatures chosen in this work were from 117.5 to 127.5 °C. The exothermal traces were recorded for the later data analysis.

An optical microscope (POM) (Olympus BX51) equipped with a temperature controller (Linkam THMS 600) was used to investigate the spherulitic morphology of neat PLLA and PLLA/MWNTs nanocomposites. The samples were first annealed at 190 °C for 3 min to erase any thermal history and then cooled to 140 °C at a cooling rate of 60 °C/min.

Wide-angle X-ray diffraction (WAXD) patterns were recorded using a Rigaku D/Max 2500 VB2t/PC X-ray diffractometer. The Cu Kα radiation ($\lambda = 0.15\,418$ nm) source was operated at 40 kV and 200 mA. WAXD patterns were recorded from 10 to 50° at 4°/min.

The hydrolytic degradation of neat PLLA and its nanocomposites were carried out in sodium hydroxide (NaOH) solution (pH = 13) at 37 °C. The degradation of neat PLLA and its nanocomposties was determined by the variation of weight loss as a function of time. The films were placed in vials filled with 10 mL of NaOH solution at 37 °C for a predetermined period of time. After hydrolysis, the films were washed with distilled water at room temperature to wipe off the NaOH solution from the surface and then dried at 70 °C under vacuum for 48 h to get the constant weight. The weight loss coefficient W_{loss} (%) was evaluated by the following relationship, i.e., W_{loss} (%) = $100 \times (W_0 - W_{t\text{-dried}})/W_0$, where W_0 is the initial weight and $W_{t\text{-dried}}$ is the weight of sample subjected to hydrolytic degradation for time t and drying in vacuum. Furthermore, the hydrolytic degradation rate R was determined by the following relationship, i.e., $R = W_{loss\text{-}t}/t$, where $W_{loss\text{-}t}$ is the weight loss and t is the exposed time in NaOH solution.[25]

Results and Discussion

Morphology and Dispersion of p-MWNTs and f-MWNTs in the PLLA Matrix. It is well-known that the dispersion of CNTs in the polymer matrix and interfacial interactions between the polymer matrix and nanotubes are the key factors influencing the physical properties of polymer matrix. A homogeneous dispersion of CNTs and strong interfacial interactions between polymer matrix and nanotubes can effectively improve the mechanical, electrical, and thermal performances of the polymer matrix. To reveal dispersion of p-MWNTs and f-MWNTs in the PLLA matrix, the fracture surfaces and ultrathin section of the nanocomposites were investigated in detail by SEM and TEM, respectively.

Parts a and b of Figure 1 show the fracture surfaces of PLLA/p-MWNTs and PLLA/f-MWNTs nanocomposties, respectively. The random dispersed bright dots and lines are the ends of the broken carbon nanotubes. For the nanocomposite containing p-MWNTs, severe aggregation of p-MWNTs is observed on the morphology as seen in Figure 1a, whereas as shown in Figure 1b individual f-MWNTs are randomly dispersed in the nanocomposite without preferred alignment or orientation, and no apparent f-MWNTs aggregation is found. The difference in the dispersion of two types of MWNTs in the PLLA matrix may be attributed to the following factors. First, the presence of electrostatic and van der Waals interactions lead to apparent aggregation of pristine MWNTs. Second, f-MWNTs possess

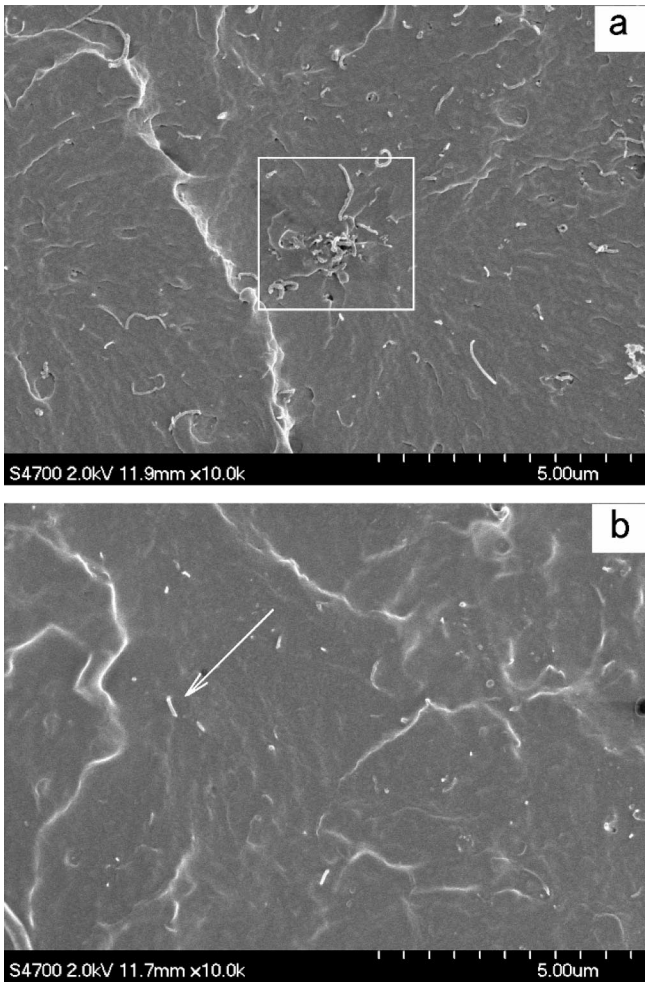

Figure 1. SEM images showing an overall morphology of surfaces for the nanocomposites: (a) PLLA/p-MWNTs and (b) PLLA/f-MWNTs.

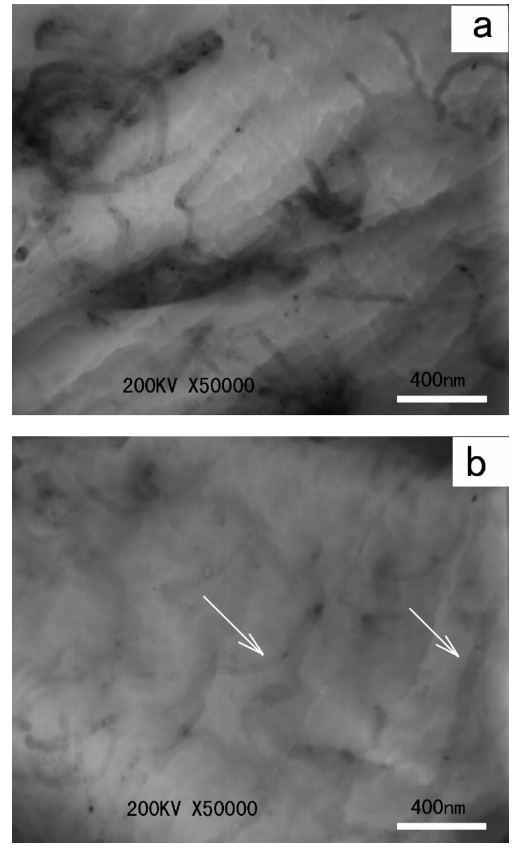

Figure 2. TEM images showing nanotubes dispersion from the ultrathin section of PLLA nanocomposites: (a) PLLA/p-MWNTs and (b) PLLA/f-MWNTs.

the carboxyl groups, which should be of great help to improve the compatibility between f-MWNTs and the PLLA matrix, preventing the severe aggregation of f-MWNTs.

In addition, it is found that most of the MWNTs are broken apart, and some MWNTs are pulled out of the matrix before the breakage. Moreover, some MWNTs are observed with their one ends still strongly embedded in the matrix. Such interesting and typical breakage phenomenon of the MWNTs indicates that a strong interfacial adhesion exists between MWNTs and PLLA matrix and that the load transfer takes place efficiently from the matrix to the nanotubes. The strong interfacial adhesion is usually responsible for the significant enhancement of the mechanical properties.[26]

Parts a and b of Figure 2 demonstrate TEM images of the ultrathin section of PLLA/p-MWNTs and PLLA/f-MWNTs nanocomposites, respectively. It is unambiguous that f-MWNTs are homogeneously dispersed in the PLLA matrix without any apparent aggregation while some aggregates are observed in the PLLA/p-MWNTs nanocomposite. Such results are consistent with SEM observations. At the same time, from Figure 2a, it is observed that most p-MWNTs remain curved in shape or even interwoven in the composite due to the extreme flexibility of the nanotubes. Similar results were also observed in the PA-6/MWNTs composites.[11] Such curvature or knotting significantly reduces the structural reinforcement of the CNTs to the host polymer matrix, in comparison to the theoretical reinforcement provided by straight inclusion.[27] However, most individual f-MWNTs are evenly dispersed in the matrix as shown in Figure 2b, which should be of great practical importance for making MWNTs reinforced PLLA nanocomposites. Both SEM and TEM observations indicate that the dispersion of f-MWNTs is better than that of p-MWNTs in the PLLA matrix; therefore, some performances of PLLA/f-MWNTs nanocomposite may be superior to those of PLLA/p-MWNTs nanocomposite.

Crystallization of PLLA before and after Nanocomposite Preparation. It is of great interest to investigate the addition of two types of MWNTs on the crystallization behavior and crystal structure of PLLA after nanocomposite preparation. As introduced in the Experimental Section, nonisothermal melt crystallization and subsequent melting of neat PLLA and its nanocomposites were studied by DSC. Figure 3a shows the DSC traces of neat PLLA and its nanocomposites cooled from the melt at 5 °C/min (first cooling). In the case of neat PLLA, a crystallization peak temperature (T_c) is found to locate at around 96.0 °C with crystallization enthalpy (ΔH_c) being around 4.2 J/g; however, in the case of nanocomposites, T_cs are found to shift to high-temperature range for both types of MWNTs. T_c is around 101.4 °C for the PLLA/p-MWNTs nanocomposite, while it is around 102.7 °C for the PLLA/p-MWNTs nanocomposite. Moreover, the values of ΔH_c of both nanocomposites are 30.5 J/g for the PLLA/p-MWNTs nanocomposite and 35.2 J/g for the PLLA/f-MWNTs nanocomposite. From the aforementioned results, it can be concluded that the incorporation of MWNTs enhances the nonisothermal melt crystallization of the PLLA matrix significantly despite the types of MWNTs. In particular, the values of ΔH_c are dramatically increased in the nanocomposites as compared with that of neat PLLA. However, T_c and ΔH_c increase very slightly in the PLLA/f-MWNTs nanocomposite compared with those in the PLLA/p-MWNTs

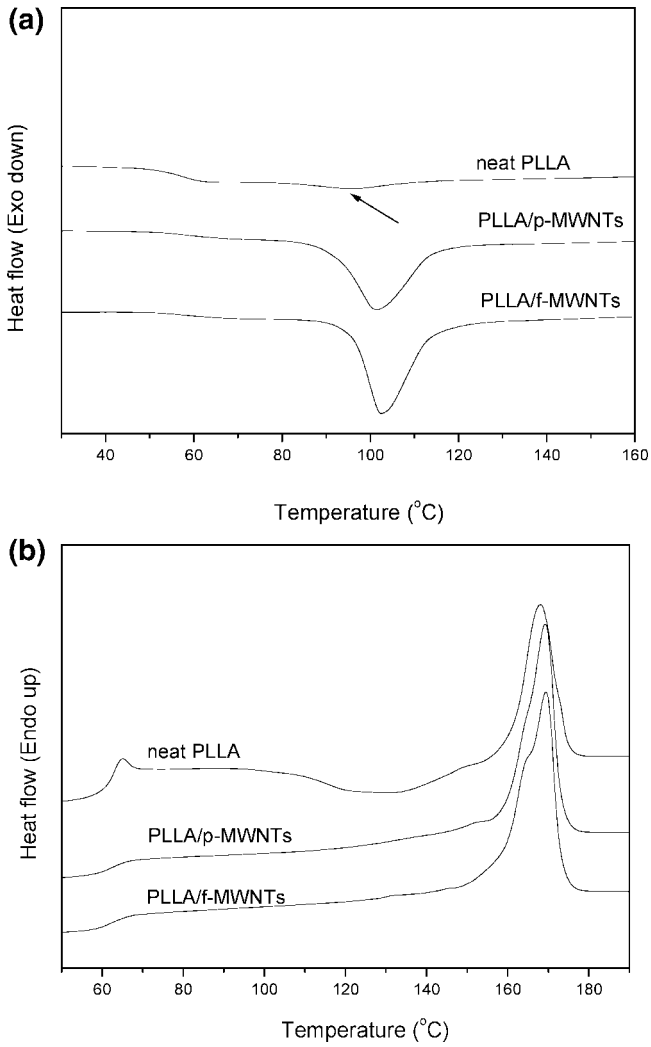

Figure 3. Nonisothermal melt crystallization and subsequent melting traces of neat PLLA and its nanocomposites: (a) first cooling and (b) second heating.

nanocomposite. Figure 3b shows the subsequent melting behavior of neat PLLA and its nanocomposites after cooling from the melt at 5 °C/min (second heating). As shown in Figure 3b, neat PLLA exhibits a glass transition temperature (T_g) of around 61.7 °C, a cold crystallization peak temperature (T_{ch}) of 132.3 °C with crystallization enthalpy (ΔH_{ch}) being 19.0 J/g, and a melting point (T_m) of 167.9 °C with heat of fusion (ΔH_m) being 24.1 J/g. The values of T_gs are around 62.5 °C in the nanocomposites and are almost unchanged before and after nanocomposites preparation. Both nanocomposites do not show cold crystallization during heating to the melt. Furthermore, the values of T_ms are around 169 °C in the nanocomposites and increase slightly as compared with that of neat PLLA. The values of ΔH_m are around 32.9 J/g for the PLLA/p-MWNTs nanocomposite and 36.6 J/g for the PLLA/f-MWNTs nanocomposite, respectively. On the basis of the heat of fusion of 100% crystalline (ΔH_m^0) PLLA (93 J/g),[28] the degrees of crystallinity (W_c) of neat PLLA and its nanocomposites are determined by the ratio of the heat of fusion of the samples to that of 100% crystalline PLLA. It should be noted that the value of cold crystallization enthalpy is subtracted from the heat of fusion in the case of neat PLLA. It is found that W_c is only around 5.5% for neat PLLA, increasing to around 35.4% and 39.4% for the PLLA/p-MWNTs nanocomposite and PLLA/p-MWNTs nanocomposite, respectively. The increase in W_c of

TABLE 1: DSC Results for the PLLA and Its Nanocomposites

sample	T_c[a] (°C)	ΔH_c[a] (J/g)	T_g (°C)	T_{ch}[b] (°C)	ΔH_{ch}[b] (J/g)	T_m (°C)	ΔH_m (J/g)	W_c[c] (%)
neat PLLA	96.0	−4.22	61.7	132.3	19.0	167.9	24.1	5.50
PLLA/p-MWNTs	101.4	−30.5	62.5	—	—	169.2	32.9	35.4
PLLA/f-MWNTs	102.7	−35.2	62.6	—	—	169.3	36.6	39.4

[a] Melt crystallization at a cooling rate of 5 °C/min (first cooling). [b] Cold crystallization at a heating rate of 20 °C/min (second heating). [c] Degree of crystallinity, W_c (%) = 100 × ($\Delta H_m - \Delta H_{ch}$)/$\Delta H_m°$.

PLLA is significant before and after nanocomposite preparation. All the DSC data are summarized in Table 1 for comparison. It is clear that the addition of MWNTs shows little effect on the variation of T_g and T_m of PLLA; however, the increase in T_c, ΔH_c, ΔH_m, and W_c is really significant. In addition, the difference in the aforementioned thermal characteristics between the PLLA/p-MWNTs and PLLA/f-MWNTs nanocomposites is very slight although f-MWNTs seem more efficient in enhancing the crystallization of PLLA than p-MWNTs.

As introduced in the Experimental Section, the overall isothermal crystallization of neat PLLA and its nanocomposites were studied by DSC in the temperature range of 117.5−127.5 °C. For all the samples, the crystallization processes prolong with the increase of crystallization temperature. In the case of the DSC experiment, the relative degree of crystallinity X_t at crystallization time t is defined as the ratio of the area under the exothermic curve between the onset crystallization time and the crystallization time t to the whole area under the exothermic curve from the onset crystallization time to the end crystallization time. Evolution of X_t with t is shown in Figure 4a for neat PLLA and its nanocomposites crystallized at 125 °C as an example. As can be seen from Figure 4a, the crystallization finishes within 37.5 min for neat PLLA while within 17.5 and 12.5 min for PLLA/p-MWNTs and PLLA/f-MWNTs nanocomposites, respectively. It is clear that the addition of MWNTs enhances the isothermal melt crystallization of PLLA compared with neat PLLA; moreover, the presence of f-MWNTs is more efficient in accelerating the crystallization process of PLLA than that of p-MWNTs.

The well-known Avrami equation is often used to analyze the isothermal crystallization kinetics;[29,30] it assumes that the relative degree of crystallinity develops with crystallization time t as

$$1 - X_t = \exp(-kt^n) \quad (1)$$

where X_t is the relative degree of crystallinity, n is the Avrami exponent depending on the nature of nucleation and growth geometry of the crystals, and k is a composite rate constant involving both nucleation and growth rate parameters. Figure 4b shows the Avrami plots of neat PLLA and its nanocomposites crystallized at 125 °C as an example. The Avrami parameters n and k can be obtained from the slopes and the intercepts, respectively. The obtained Avrami parameters of neat PLLA and its nanocomposites are summarized and listed in Table 2.

From Table 2, it can be seen that the average values of Avrami exponent n are around 2.3 for neat PLLA, 2.4 for the PLLA/p-MWNTs nanocomposite, and 2.8 for the PLLA/f-MWNTs nanocomposite, respectively. The incorporation of MWNTs does not affect the Avrami exponents significantly, indicating that the crystallization mechanism may not change. The DSC results reported herein are consistent with the spherulitic morphology and growth studies in the following

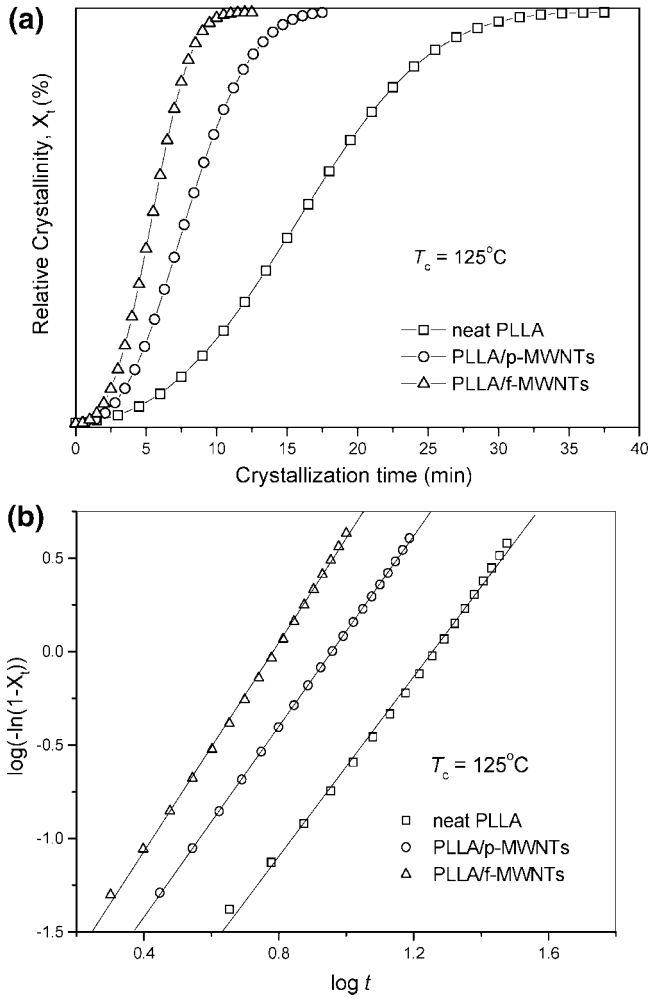

Figure 4. Effect of p-MWNTs and f-MWNTs on the crystallization of PLLA at 125 °C: (a) development of relative crystallinity with crystallization time and (b) the Avrami plots.

TABLE 2: Crystallization Kinetic Parameters for Neat PLLA and Its Nanocomposites

samples	T_c (°C)	n	k (min^{-n})	$t_{0.5}$ (min)	$1/t_{0.5}$ $(min)^{-1}$
neat PLLA	117.5	2.3	1.94×10^{-2}	4.79	0.209
	120.0	2.2	8.92×10^{-3}	7.01	0.143
	122.5	2.5	1.55×10^{-3}	11.3	0.089
	125.0	2.4	9.57×10^{-4}	15.0	0.067
	127.5	2.3	7.19×10^{-4}	19.9	0.050
PLLA/p-MWNTs	117.5	2.3	9.97×10^{-2}	2.30	0.435
	120.0	2.7	1.85×10^{-2}	3.81	0.262
	122.5	2.3	1.71×10^{-2}	4.92	0.203
	125.0	2.6	3.75×10^{-3}	7.74	0.129
	127.5	2.3	2.83×10^{-3}	10.5	0.095
PLLA/f-MWNTs	117.5	2.6	1.27×10^{-1}	1.90	0.526
	120.0	2.8	3.98×10^{-2}	2.74	0.365
	122.5	2.9	1.33×10^{-2}	3.99	0.251
	125.0	2.7	7.82×10^{-3}	5.11	0.196
	127.5	2.9	3.16×10^{-3}	6.49	0.154

section. On the other hand, the values of the crystallization rate k decrease with increasing crystallization temperature for both neat PLLA and its nanocomposites, indicating that the crystallization process is nucleation controlled because of the low supercooling. For a given crystallization temperature, the values of k increase after nanocomposites preparation as compared with that of neat PLLA; moreover, the value of k for the PLLA/f-MWNTs nanocomposite is greater than that of PLLA/p-MWNTs nanocomposite, indicating that f-MWNTs are more efficient in enhancing the isothermal melt crystallization in the nanocomposite than p-MWNTs. The increase in the values of k suggests that the incorporation of MWNTs accelerates the overall crystallization process of PLLA in the nanocomposites as compared with neat PLLA, which should be attributed to the heterogeneous nucleation effect of MWNTs on the crystallization of PLLA.[31]

The half-life crystallization time $t_{0.5}$, the time required to achieve 50% of the final crystallinity of the samples, is an important parameter for the discussion of crystallization kinetics. The value of $t_{0.5}$ is calculated by the following equation:

$$t_{0.5} = \left(\frac{\ln 2}{k}\right)^{1/n} \tag{2}$$

Usually, the crystallization rate can also be easily described by the reciprocal of $t_{0.5}$. The values of $t_{0.5}$ and $1/t_{0.5}$ are thus calculated through eq 2 and listed in Table 2, too. For all the three samples, with increasing T_c the values of $t_{0.5}$ increase while the values of $1/t_{0.5}$ decrease. Such variations indicate that the overall isothermal crystallization rate decrease with the increase of T_c. The slow-down of the overall crystallization rate with increasing T_c may be attributed to the fact that the isothermal melt crystallization investigated in this work is a nucleation controlled process because of the low supercooling. Furthermore, the values of $t_{0.5}$ for the nanocomposites are smaller than those of neat PLLA at a given T_c; on the other hand, the values of $1/t_{0.5}$ for the nanocomposite are larger than those of neat PLLA, indicating again that after nanocomposites preparation with MWNTs the crystallization process of PLLA is accelerated.

It is clear from Table 2 that the overall crystallization rate is faster for the nanocomposite prepared with f-MWNTs than that prepared with p-MWNTs. The difference in the overall crystallization rate may be related to the following factors. Although both p-MWNTs and f-MWNTs act as nucleating agent for the crystallization of PLLA in the nanocomposites, the nucleation ability and the influence on the overall crystallization process are different. It is expected that the spherulites start to grow earlier, but their growth will be hindered by the presence of the aggregates of MWNTs. However, the surface energy of MWNTs is so high that they are easily to aggregate, especially for those without functional groups. The aggregated MWNTs not only give rise to a poor distribution but also make themselves less effective as nucleating agents in enhancing the crystallization of PLLA. In the present work, the dispersion of f-MWNTs is much better than that of p-MWNTs throughout the PLLA matrix as evidenced by SEM and TEM observations in the previous section. Therefore, f-MWNTs are more effective as a nucleation agent to enhance the crystallization of PLLA than p-MWNTs due to the presence of functional carboxyl groups on the side walls.

The effect of the presence of MWNTs on the spherulitic morphology of PLLA was studied by POM. Figure 5 shows the spherulitic morphology of neat PLLA and its nanocomposites crystallized at 140 °C. Well-developed spherulites grow to a size of roughly 200 μm in diameter in the case of neat PLLA. Although the morphology of PLLA seems to be obscure because of low supercooling, clear boundaries can easily be seen as shown in Figure 5a. Parts b and c of Figure 5 illustrate the POM images of PLLA spherulites after nanocomposites preparation with p-MWNTs and f-MWNTs, respectively. It is clear that the size of PLLA spherulites becomes smaller in the presence of MWNTs, indicative of the increase of nucleation density. In

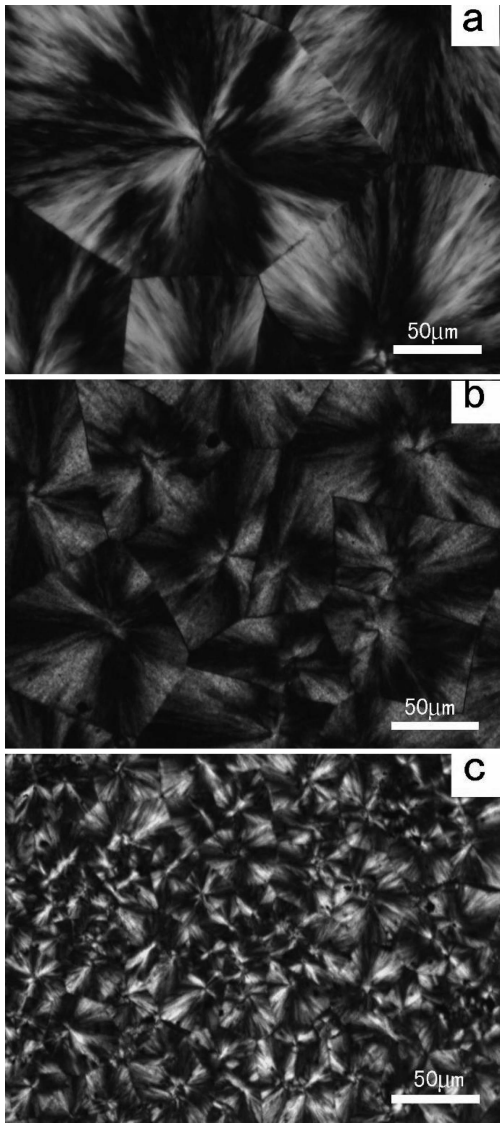

Figure 5. Spherulitic morphologies of (a) neat PLLA, (b) PLLA/p-MWNTs, and (c) PLLA/f-MWNTs crystallized at 140 °C by POM.

particular, in the case of PLLA/f-MWNTs nanocomposite some smaller and imperfect spherulites with diameter less than 50 μm are observed to grow rapidly, impinge quickly with surrounding spherulites, and restrict further growth. Spherulitic morphology studies indicate that the nucleation density of PLLA is improved due to the presence of MWNTs in the nanocomposites and f-MWNTs seem more effective as a nucleation agent than p-MWNTs in the crystallization process of PLLA, which are consistent with the DSC results in the previous section. These results reveal clearly that a good dispersion of f-MWNTs in the PLLA matrix influences efficiently the spherulitic morphology and the overall crystallization process of PLLA.

It is of great interest to study the effect of the incorporation of MWNTs on the crystal structure of PLLA in the nanocomposites. Figure 6 illustrates the WAXD patterns of neat PLLA and its nanocomposites, which were crystallized at 125 °C for one day. Three crystal modifications, including α, β, and γ forms, have been reported for PLLA, and crystallization from the melt usually leads to α form, which is the most common polymorph.[32,33] In the present work, the samples for the WAXD measurements were crystallized at 125 °C; therefore, neat PLLA and its nanocomposites should crystallize in α form. As shown

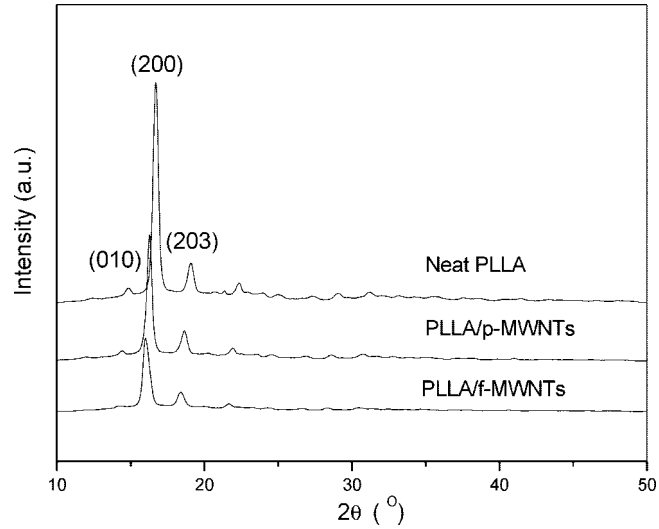

Figure 6. WAXD patterns of neat PLLA and its nanocomposites.

TABLE 3: WAXD Data for Neat PLLA and Its Nanocomposites

samples	d_{010} (nm)	d_{200} (nm)	d_{203} (nm)	a (nm)	b (nm)	c (nm)	V (nm^3)
neat PLLA	0.596	0.530	0.466	1.061	0.596	2.919	1.845
PLLA/p-MWNTs	0.613	0.543	0.476	1.087	0.613	2.964	1.974
PLLA/f-MWNTs	0.628	0.553	0.482	1.106	0.628	2.961	2.054

in Figure 6, neat PLLA shows three main characteristic diffraction peaks at around 14.86°, 16.70°, and 19.04°, corresponding to (010), (200), and (203), respectively.[32,33] In the case of the nanocomposites, the diffraction peaks shift slightly to the lower angle as compared with those of neat PLLA, indicating that the corresponding interplanar spacings increase with the addition of MWNTs. The related values of interplanar spacing for neat PLLA and its nanocomposites are summarized in Table 3, which increase slightly with the addition of MWNTs. Moreover, the intensities of the diffraction peaks of PLLA are reduced apparently after nanocomposites preparation, indicative of a decrease in degree of crystallinity and a gradual decrease in crystalline order.

Since in the α form two chains with 10_3 helical conformation are packed into orthorhombic unit cell for PLLA, the unit cell with dimensions a, b, and c can be obtained from the interplanar spacings shown in Table 3 through the following equation

$$\frac{1}{d_{hkl}^2} = \frac{h^2}{a^2} + \frac{k^2}{b^2} + \frac{l^2}{c^2} \tag{3}$$

The obtained unit cell dimensions and the corresponding unit cell volume are listed in Table 3, too. Similar to the increase trend in the interplanar spacing, both the unit cell dimensions and volume expand in the presence of MWNTs as compared with those of neat PLLA; furthermore, f-MWNTs seems more efficient in expanding the unit cell dimensions and volume than p-MWNTs although the difference is very limited. Therefore, the addition of MWNTs makes the crystallization of PLLA easier to start but also hinders the extent of crystallization and thus the ultimate extent of bulk crystallinity. In brief, nanocomposites preparation with MWNTs does not modify the crystal structure but reduces the ultimate extent of bulk crystallinity of PLLA after crystallization at 125 °C for even enough crystallization time.

Hydrolytic Degradation. The addition of MWNTs on the hydrolytic degradation of PLLA is of great interest. In this

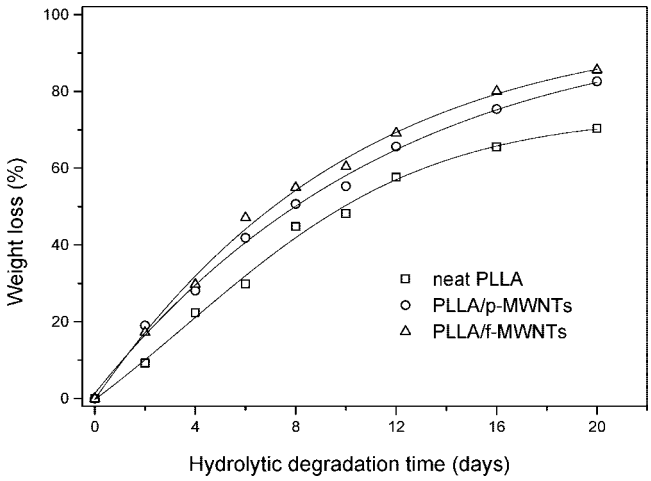

Figure 7. Variation of weight loss with hydrolytic degradation time for neat PLLA and its nanocomposites.

section, the hydrolytic degradation of neat PLLA and its nanocomposites were studied by measuring the weight loss of PLLA as a function of exposed time in NaOH solution at 37 °C. Figure 7 shows the variation of weight loss of neat PLLA and its nanocomposites with exposed time in hydrolysis test. The values of weight loss increase with prolonging exposed time for both neat PLLA and its nanocomposites. As shown in Figure 7, the almost linear variation of weight loss with exposed time is observed in the early stage when the time is within around 6 days. Therefore, the hydrolytic degradation rates of neat PLLA and its nanocomposites can be obtained from the initial slopes of the plots of weight loss against exposed time, which are around 5.13 ± 0.36%/day for neat PLLA, 6.73 ± 0.66%/day for PLLA/p-MWNTs nanocomposite, and 7.69 ± 0.33%/day for PLLA/f-MWNTs nanocomposite, respectively. It is clear that the hydrolytic degradation rates of the nanocomposites with MWNTs are faster than that of neat PLLA, indicating that the addition of MWNTs accelerates the hydrolytic degradation of PLLA after nanocomposites preparation; moreover, the hydrolytic degradation rate of PLLA/f-MWNTs nanocomposite is slightly faster than that of PLLA/p-MWNTs nanocomposite, although the difference in the hydrolytic degradation rate is very limited between the two nanocomposites. With further prolonging the exposed time in NaOH solution, the values of weight loss continue to increase; however, the hydrolytic degradation rates become slower in the later stage than in the early stage as evidenced from the difference between the slopes of the early and the later stages because the amorphous phase is easy to degrade compared with that of the crystal phase.[34] The ultimate values of the weight loss reach around 70.3% for neat PLLA, around 82.0% for PLLA/p-MWNTs nanocomposite, and around 85.6% for PLLA/f-MWNTs nanocomposite, after 20 days exposed time in NaOH solution as shown in Figure 7.

The exciting aspect of this research is the enhanced hydrolytic degradation of PLLA after nanocomposites preparation with MWNTs as evidenced from the aforementioned results. It is well-known that two kinds of factors affect the degradation of aliphatic polyesters.[35−38] One is various environmental factors such as pH, temperature, and buffer composition, etc. The other is internal factors such as crystallinity and morphology. In the present work, the same environmental conditions were used in studying the hydrolytic degradation. Therefore, the difference in the hydrolytic degradation must come from the internal factors. Crystallinity is an important factor influencing the degradation of PLLA since the crystal phase is more difficult to degrade as compared with that of the amorphous phase. As introduced in the Experimental Section, the films for the hydrolytic degradation test were prepared by hot molding followed by cooling naturally to room temperature. The values of crystallinity are estimated from a first heating at 20 °C/min in a DSC experiment, which are determined to be around 15.3%, 37.4%, and 38.1% for neat PLLA, PLLA/p-MWNTs, and f-MWNTs nanocomposites, respectively. However, the hydrolytic degradation rates are faster in the nanocomposites than in neat PLLA although the values of degree of crystallinity are higher in the nanocomposites than that of neat PLLA, indicating that the crystallinity is not the controlling factor in affecting the hydrolytic degradation of PLLA before and after nanocomposites preparation with MWNTs in the present work. Actually, similar results were also found by Okamoto et al. for the biodegradability study of PLLA and layered silicate nanocomposites.[39] In the case of PLLA/layered silicate nanocomposites, the crystallinity of neat PLLA is lower than those of nanocomposites while the biodegradation rates of the latter are faster than that of the former. The enhanced biodegradation rate of PLLA/layered silicate nanocomposites is attributed to a different mode of attack on the PLLA component of the test samples due to the presence of different kinds of modified salts and pristine silicates.[39] Therefore, it is also conceivable that the incorporation of MWNTs into the PLLA matrix in the present work may result in a different mode of attack on the PLLA component and a different mode of disruption of some of the ester linkages due to the presence of different types of MWNTs. The exact degradation mechanism of PLLA/MWNTs nanocomposites needs further investigation and will be reported in the forthcoming work. In brief, nanocomposites preparation with MWNTs enhances the hydrolytic degradation of PLLA, which may be of great interest for its wide practical application as packing materials and biomaterials.

Conclusions

Biodegradable PLLA/MWNTs nanocomposites have been prepared with p-MWNTs and f-MWNTs in this work. Severe aggregation of p-MWNTs is observed in the PLLA matrix by SEM and TEM, whereas f-MWNTs show a fine and homogeneous dispersion in the nanocomposite, indicating that functionalization of MWNTs is an effective way in improving the dispersion in the polymer matrix. Nonisothermal crystallization behavior and isothermal crystallization kinetics studies indicate that the presence of MWNTs enhances the crystallization of PLLA in the nanocomposites compared with that of neat PLLA, which should be attributed to the strong heterogeneous nucleation of MWNTs. Furthermore, f-MWNTs seem to be more efficient as a nucleating agent than p-MWNTs due to the better and homogeneous dispersion of the former in the PLLA matrix. Spherulitic morphology studies of neat PLLA and its nanocomposites confirm that the nucleation density of PLLA in the presence of f-MWNTs is higher than that in the p-MWNTs, which is consistent with the DSC study. Furthermore, it is found that the crystal structures of PLLA do not change after nanocomposites preparation but the corresponding unit cell dimensions and volume expand after crystallizing isothermally at 125 °C for a given enough time. The exciting aspect of this research is the enhanced hydrolytic degradation of PLLA after nanocomposites preparation with MWNTs, which might be of great interest for its wide practical application as packing materials and biomaterials.

Acknowledgment. The authors thank Biomer, Germany, for kindly providing PLLA samples. Part of this work is financially supported by the National Natural Science Foundation, China (Grant Nos. 20504004 and 20774013), Program for New Century Excellent Talents in University (NCET-06-0101), and Program for Changjiang Scholars and Innovative Research Team in University (IRT0706).

References and Notes

(1) Iijima, S. *Nature* **1991**, *354*, 56.
(2) Gao, G.; Cagin, T.; Goddard, W. A. *Nanotechnology* **1998**, *9*, 184.
(3) Uchida, T.; Kumar, S. *J. Appl. Polym. Sci.* **2005**, *98*, 985.
(4) Walt, D.; Heer, A. *MRS Bull.* **2004**, *29*, 281.
(5) Tans, S. J.; Devoret, M. H.; Dai, H.; Thess, A.; Smalley, R. E.; Geerligs, L. J.; Dekker, C. *Nature* **1997**, *386*, 474.
(6) Berber, S.; Kwon, Y. K.; Tomanek, D. *Phys. Rev. Lett.* **2000**, *84*, 4613.
(7) Moniruzzaman, M.; Winey, K. I. *Macromolecules* **2006**, *39*, 5194.
(8) Haggenmueller, R.; Fischer, J. E.; Winey, K. I. *Macromolecules* **2006**, *39*, 2964.
(9) Levi, N.; Czerw, R.; Xing, S.; Iyer, P.; Carroll, L. D. *Nano Lett.* **2004**, *4*, 1267.
(10) Chen, G. X.; Shimizu, H. *Polymer* **2008**, *49*, 943.
(11) Liu, T. X.; Phang, I. Y.; Shen, L.; Chow, S. Y.; Zhang, W. D. *Macromolecules* **2004**, *37*, 7214.
(12) Li, X.; Huang, Y. D.; Liu, L.; Cao, H. L. *J. Appl. Polym. Sci.* **2006**, *102*, 2500.
(13) Chen, S. M.; Wu, G. Z.; Liu, Y. D.; Long, D. W. *Macromolecules* **2006**, *39*, 330.
(14) Li, J.; Fang, Z. P.; Zhu, Y.; Tong, L. F.; Gu, A. J.; Liu, F. *J. Appl. Polym. Sci.* **2007**, *105*, 3531.
(15) Ke, G.; Guan, W.; Tang, C.; Guan, W.; Zeng, D.; Deng, F *Biomacromolecules* **2007**, *8*, 322.
(16) Lai, M. F.; Li, J.; Yang, J.; Liu, J.; Tong, X.; Cheng, H. M. *Polym. Int.* **2004**, *53*, 1479.
(17) Wang, S. F.; Shen, L.; Zhang, W. D.; Tong, Y. J. *Biomacromolecules* **2005**, *6*, 3067.
(18) Yoon, S. H.; Jin, H. J.; Kook, M. C.; Pyun, Y. R. *Biomacromolecules* **2006**, *7*, 1280.
(19) Drumright, R. E.; Gruber, P. R. *Adv. Mater.* **2000**, *12*, 1841.
(20) Moon, S.; Jin, F. Z.; Lee, C. J.; Tsutsumi, S.; Hyon, S. H. *Macromol. Symp.* **2005**, *224*, 287.
(21) Zhang, D. H.; Kandadai, M. A.; Cech, J.; Roth, S.; Curran, S. A. *J. Phys. Chem. B* **2006**, *110*, 12910.
(22) Wu, C. S.; Liao, H. T. *Polymer* **2007**, *48*, 4449.
(23) Shieh, Y. T.; Liui, G. L. *J. Polym. Sci.: Part B: Polym. Phys.* **2007**, *45*, 1870.
(24) Kim, H. S.; Park, B. H.; Yoon, J. S.; Jin, H. J *Eur. Polym. J.* **2007**, *43*, 1729.
(25) Shirahase, T.; Komatsu, Y.; Tominaga, Y.; Asai, S.; Sumita, M. *Polymer* **2006**, *47*, 4839.
(26) Chen, G. X.; Kim, H. S.; Park, B. H.; Yoon, J. S. *Polymer* **2006**, *47*, 4760.
(27) Fisher, F. T.; Bradshaw, R. D.; Brinson, L. C. *Appl. Phys. Lett.* **2002**, *80*, 4647.
(28) Fisher, E. M.; Sterzel, H. J.; Wegner, G. *Kolloid Z. Z. Polym.* **1973**, *251*, 980.
(29) Avrami, M. *J. Chem. Phys.* **1939**, *7*, 1193.
(30) Avrami, M. *J. Chem. Phys.* **1940**, *8*, 212.
(31) Sinha Ray, S.; Vaudreuil1, S.; Maazouz, A.; Bousmina, M. *J. Nanosci. Nanotechnol.* **2006**, *6*, 2191.
(32) De, S. P.; Kovacs, A. J. *Biopolymers* **1968**, *6*, 299.
(33) Kawai, K.; Rahman, N.; Matsuba, G.; Nishida, K.; Kanaya, T.; Nakano, M.; Okamoto, H.; Kawada, J.; Usuki, A.; Honma, N.; Nakajima, K.; Matsuda, M. *Macromolecules* **2007**, *40*, 9463.
(34) Iwata, T.; Doi, Y. *Macromolecules* **1998**, *31*, 2461.
(35) Andrianov, A. K.; Marin, A. *Biomacromolecules* **2006**, *7*, 1581.
(36) Scandola, M.; Focarete, M. L.; Adamus, G.; Sikorska, W.; Baranowska, I.; Swierczek, S.; Gnatowski, M.; Kowalczuk, M.; Jedlinski, Z. *Macromolecules* **1997**, *30*, 2568.
(37) Tomasi, G.; Scandola, M.; Briese, B. H.; Jendrossek, D. *Macromolecules* **1996**, *29*, 507.
(38) Kikkawa, Y.; Suzuki, T.; Tsuge, T.; Kanesato, M.; Doi, Y.; Abe, H *Biomacromolecules* **2006**, *7*, 1921.
(39) Sinha Ray, S.; Okamoto, M. *Macromol. Rapid Commun.* **2003**, *24*, 815.

JP805230E